Construction and Building Materials 260 (2020) 120438

Contents lists available at ScienceDirect

Construction and Building Materials

journal homepage: www.elsevier.com/locate/conbuildmat

Study of the permanent deformation of binders and asphalt mixtures using rheological models of fractional viscoelasticity

M. Lagos-Varas [a,b,*], A.C. Raposeiras [a], D. Movilla-Quesada [a], J.P. Arenas [c], D. Castro-Fresno [b], O. Muñoz-Cáceres [a,b], V.C. Andres-Valeri [a]

[a] Gi²V Research Group, Institute of Civil Engineering, Faculty of Engineering Sciences, Univ. Austral of Chile, Valdivia, Chile
[b] GITECO Research Group, Dept. of Transportation and Technology of Projects and Processes, University of Cantabria, 39005 Santander, Spain
[c] Institute of Acoustics, Faculty of Engineering Sciences, Univ. Austral of Chile, PO Box 567, Valdivia, Chile

GRAPHICAL ABSTRACT

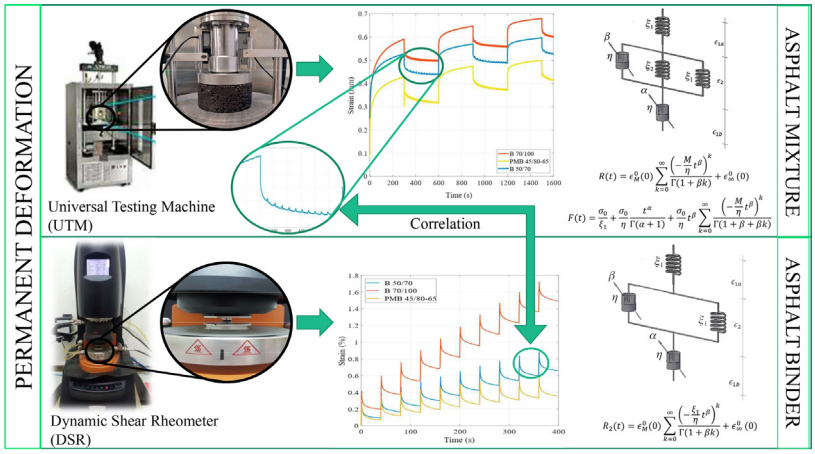

ARTICLE INFO

Article history:
Received 29 January 2020
Received in revised form 28 May 2020
Accepted 30 July 2020
Available online 30 August 2020

Keywords:
Permanent deformation
Rheological properties
MSCR
Viscoelastic
Creep-recovery
Asphalt binder

ABSTRACT

The accumulation of load on asphalt pavement as a result of increased vehicle traffic generates problems in the asphalt layer due to permanent deformation. For correct design, it is essential to carry out a rheological characterization of the aggregate-binder materials that make up the asphalt mix. This article shows the analysis of permanent deformation based on the rheological behavior of asphalt mixtures and binders. Experimental tests based on creep and recovery phenomena allow the study of permanent deformations using theoretical models of fractional viscoelasticity. The rheological characterization allows us to detail the elasticity of the aggregate, ξ_2, and the elastic-viscous properties of the different binders used, ξ_1 and η. The results obtained show that it is possible to predict the deformations of the recovery phenomenon in asphalt mixtures from the rheological values (aggregate-binder) obtained in the creep process. Besides, the properties of the asphalt binder (ξ_1 and η) correlate with the recovery phenomenon of the MSCR test for conventional and modified materials. The methodology proposed allows a better understanding of the states of permanent deformation to improve the design of binders and asphalt mixtures.

* Corresponding author at: Institute of Civil Engineering, Universidad Austral de Chile, 2086 Valdivia, Chile.
E-mail address: manuel.lagos@uach.cl (M. Lagos-Varas).

https://doi.org/10.1016/j.conbuildmat.2020.120438
0950-0618/

1. Introduction

Asphalt mixtures have for decades been the most commonly used composite material for the construction of flexible pavements [1]. The use of mineral aggregate and asphalt binder as the skeleton and agglomerate of the asphalt mix has made it possible to ensure the quality and comfort of the road structure for controlled periods. However, the increase in vehicle traffic and tremendous climatic variations have caused permanent damage to the asphalt layers along the path of the wheels, resulting in traffic accidents due to the poor quality and comfort of driving [2].

The asphalt binder is a petroleum-based product that has little elastic capacity when subjected to different stresses, generating plastic deformations due to its viscoelastic nature [3]. Therefore, in recent decades, the rheological study of this material has generated great scientific discussions and comparisons on its mechanical behavior in the asphalt mix. The rheological analysis generates various methodologies that establish parameters for different static and dynamic stresses. The methodology proposed by Superpave for tests on asphalt binders using a dynamic shear rheometer (DSR) makes it possible to establish a limit with the parameter $G^*/sen(\delta)$ to predict the failure of permanent deformations in asphalt mixture [4–6]. However, the technological advance of new binder-modifying materials and asphalt mixtures, such as oils, waxes, polymers, among other materials [7–10], do not generate an adequate representation of permanent deformation since it known that Superpave parameters are focused on linear viscoelastic deformation [11]. In this case, the pavement will be designed to be able to withstand the stresses and strains of the traffic, which are not reflected in the deformations caused by rutting, since these occur in a non-linear viscoelastic range. For this reason, the Federal Highway Administration (FHWA) has conducted studies based on the phenomenon of multiple stress creep recovery (MSCR) to understand the ability of the asphalt binder to recover some initial deformation [12], generating a complementary test for the rheological analysis of asphalt binders. The studies based on the analysis of these phenomena mention that the MSCR test characterizes the properties of the asphalt binder in a different way than the DSR-test [12] due to the different levels of loading and natures of the tests [13]. In this sense, the MSCR is a test that is more related to the rutting performance of the asphalt mix, reaching greater detail on the behavior in base and polymer binders [14] and evaluating the modification efficiency rate of additives and modifiers in asphalt binders [15].

Creep and recovery phenomena generate with static cycles in controlled time intervals [16]. The creep phenomenon is the deformation that occurs in the process of loading the material, which generates elastic-viscous strains that depend on different factors such as the test temperatures, load magnitude, or nature of the load [17,18]. Subsequently, the recovery phenomenon details the capacity of the material to redeem the deformations obtained in the creep process and to avoid the complete plastic deformation of the binder or asphalt mix [19]. The behavior exhibited by the asphalt mix and binder is complemented by experimental analysis with numerical models that allow understanding of permanent deformations, generating various methodologies that address the phenomena of creep and recovery.

In the literature, several models allow the establishment of rheological values for elastic-viscous deformations. The fractional Burgers model proposed by Oeser requires four parameters to describe the progressive deformation of an asphalt binder [20]. This model allows the correct adoption of the deformations of a viscoelastic material from its elastic to a viscous state, but it was not a solution when submitted to the analysis of composite materials such as an asphalt mix (aggregate-binder). The use of the aggregate-binder matrix as a single material does not allow the elastic-viscous transitions of the asphalt binder to be detailed independently. Therefore, one of the disadvantages of rheological characterization by these mechanical models is that it is hard to control the variability or uncertainty of the experimental tests, resulting from the complex mechanical and environmental variations in the laboratories [21]. In this regard, some research claims that no single model commonly used in the literature is ideal for predicting asphalt mix deformation, as they all have several disadvantages, such as predicting creep and recovery deformation with a single model [20].

Consequently, in previous studies [20] a rheological model was proposed to determine the viscoelastic deformations of asphalt mixtures, for creep, recovery, and relaxation phenomena while maintaining the rheological properties of the aggregate and asphalt binder as a whole. In this sense, the proposed model establishes a set of springs and dampers, which jointly and/or separately represent the elastic deformations of the mineral aggregate (aggregate) and viscoelastic deformations of the asphalt binder (see Fig. 1). The mathematical study was determined using fractional differential equations, which generate operators to represent the rheological transition from the elastic to the viscous state of the asphalt binder [22]. In this way, the present study introduces a correlation of the creep-recovery deformations that occur in the MSCR with those in asphalt mixtures which is important for determining the viscoelastic behavior of the binder. Thus, determining the elastic properties of the aggregate skeleton and the influence caused by the plastic capacity of asphalt binders.

The first spring represents the critical point of linear viscoelasticity (see Fig. 1, phase 1). Then, the change of curvature gives rise to the nonlinear viscoelasticity (see Fig. 1, phase 2) and corresponds to the complete system (aggregate-binder); the material is still in the stage of no plastic damage, acting at the same time as the elasticity of the aggregate. The last state of the creep phenomenon, or the plastic damage stage (see Fig. 1, stage 3), is determined by a fractional damper, which indicates the final deformation from which the mixture will not be able to recover. The recovery phenomenon begins with an initial instantaneous strain defined by a fit factor from Maxwell's model. Subsequently, the model allows for detailing the recovery curve with the same rheological properties obtained from the creep phenomenon to determine the projection of the permanent deformation curves.

The objective of this study is to optimize the asphalt mix design methodology for states of permanent deformation based on a rheological correlation of the properties of the asphalt mix and asphalt binder. The methodology proposed allows us to distinguish the rheological properties of the aggregate-binder materials. The equations were obtained using fractional order derivatives and were implemented into computer codes using MATLAB©.

2. Materials and methods

2.1. Asphalt binder and aggregate

Conventional (B50/70 and B70/100) and modified (PMB 45/80-65) asphalt binders are used in this study. The properties of the asphalt binders are shown in Table 1. Regarding the mineral skeleton, ophitic aggregate is used for coarse, fine, and filler sizes. This material is used in surface layers due to its anti-slip and wear-resistance qualities, ensuring the necessary surface texture for a given time. The properties of the mineral aggregate are shown in Table 2 [23].

In this study, three types of asphalt mixes were used to verify the proposed mechanical models. For each type of mixture, 16

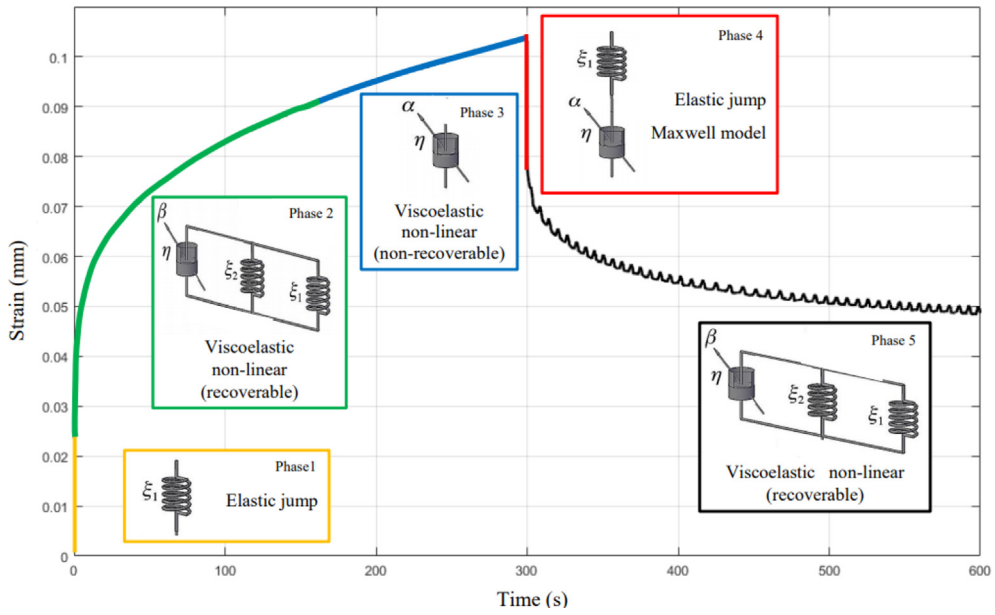

Fig. 1. Representative diagram of the phenomena of creep and recovery.

Table 1
Properties of the asphalt binders.

	Units	Standard	Binder		
			B50/70	B70/100	PMB45/80-65
Penetration at 25 °C	0.1 mm	EN 1426	57.0	70.0	49.5
Softening point R&B	°C	EN1427	51.6	48.5	72.3
Fraass breaking point	°C	EN 12593	−13.0	−10.0	−13.0
Density at 25 °C	G cm^{-3}	EN 15326	1.035	1.020	1.030

Table 2
Properties of the ophitic aggregate.

	Units	Standard	Ophitic aggregate
Bulk density	g/cm^3	EN 1097-6	2,725
Los Angeles coefficient	%	EN 1097-2	15
Flakiness Index	%	EN 933-3	8
Resistance to polishing	%	EN 1097-8	56

Marshall samples with a diameter of 101.6 mm and a height of 65 mm were manufactured, with a compaction number of 75 blows per side. A semi-dense asphalt mix type AC16S was selected, with 5 wt% content of binder. Samples were manufactured at 153 °C for conventional binders B50/70 and B70/100, and samples with PBM45/80-65 were produced at 165 °C. Four equal samples for each type of asphalt binder were selected.

2.2 . Creep and recovery of asphalt mixtures

The creep and uniaxial static recovery tests were carried out using the universal testing machine (UTM) for asphalt mixtures at different temperatures and load frequencies (see Fig. 2a). The permanent deformation of the material was determined at a predetermined constant load within a set period of 10 min [21]. The test temperature was set at 20 °C since under this condition the three asphalt binders have an approximate offset of 50° with respect to the load which causes variable deformation rates over time [3].

2.3 . Multiple stress creep recovery (MSCR) for asphalt binders

The multiple stress creep and recovery (MSCR) test was performed on the dynamic shear rheometer (DSR) for conventional and modified binders (see Fig. 2b). The deformation of the samples was determined for a temperature of 20 °C, developing 10 continuous load-unload cycles. The load was determined for deformation of 0.1% in 1 s, and the recovery time was extended up to 39 s.

2.4. Rheological model for asphalt mixtures

The model proposed for asphalt mixtures allows the characterization of the rheological properties of aggregate-binder materials. The representation of the asphalt mixes was based on an aggregate particle covered in a continuous film of asphalt binder, i.e., an elastic element surrounded by an elastic-viscous assembly [20]. The properties of the mineral aggregate and the different types of asphalt binders are obtained using the equations that describe the creep and recovery phenomena. In this regard, the methodology proposed (see Fig. 3) begins with curve-fitting the deformations occurring in the creep phenomenon of asphalt mixtures, i.e., Eq. (1). Subsequently, the curve-fitting for the recovery phenomenon, i.e., Eq. (2) is carried out with the same rheological values obtained in the previous process, to cover the complete loading–unloading cycle in asphalt mixtures. The equations for the creep and recovery are, respectively,

$$F(t) = \frac{\sigma_0}{\xi_1} + \frac{\sigma_0}{\eta}\frac{t^{\alpha}}{\Gamma(\alpha+1)} + \frac{\sigma_0}{\eta}t^{\beta}\sum_{k=0}^{\infty}\frac{\left(-\frac{M}{\eta}t^{\beta}\right)^{k}}{\Gamma(1+\beta+\beta k)}, \quad (1)$$

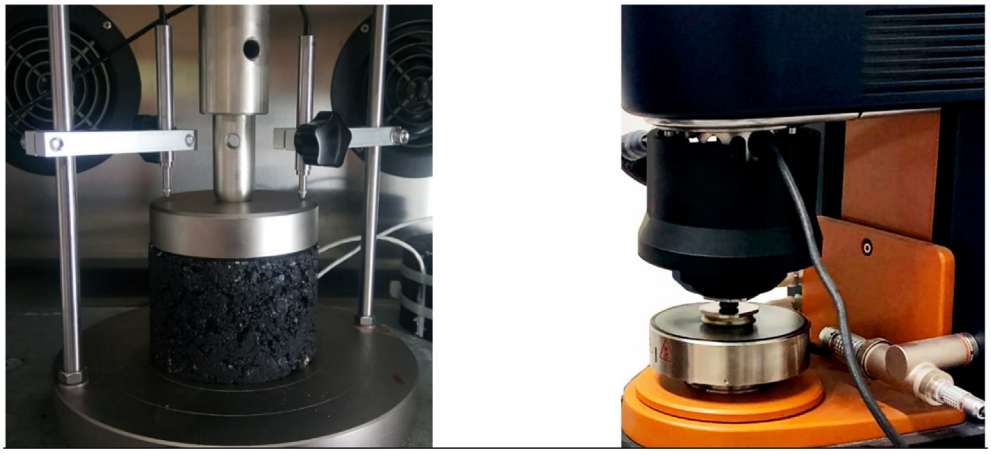

Fig. 2. Creep and recovery tests. a) Asphalt mixture; b) Asphalt binder.

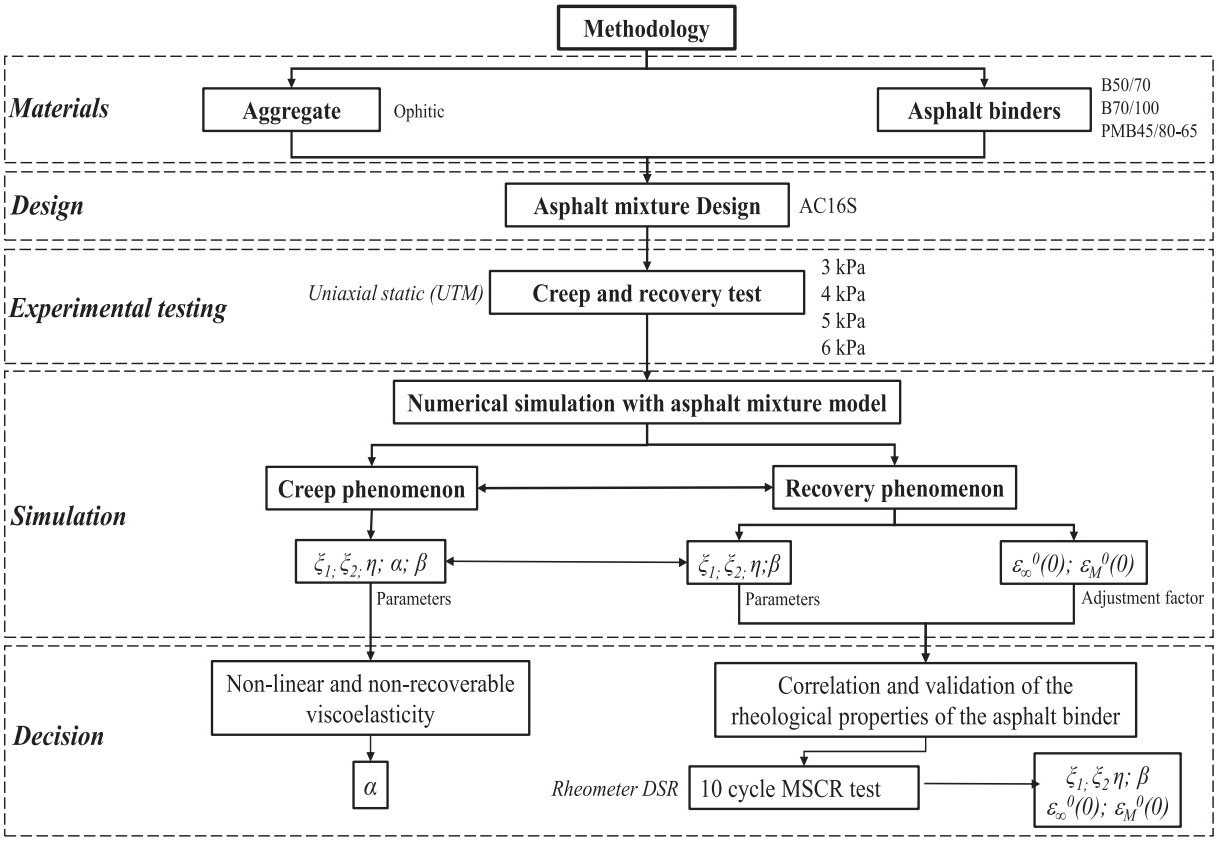

Fig. 3. Schematic of the methodology for determining the properties of the mineral aggregate and the different types of asphalt binders.

$$R(t) = \epsilon_M^0(0)\sum_{k=0}^{\infty}\frac{\left(-\frac{M}{\eta}t^{\beta}\right)^k}{\Gamma(1+\beta k)} + \epsilon_{\infty}^0(0), \tag{2}$$

where $F(t)$ is the creep deformation, $R(t)$ is the recovery deformation, $M = \xi_2 + \xi_1$ is the elastic property of the asphalt mix, ξ_2 is the elasticity of aggregate, ξ_1 and η are the elastic and viscous constants of the asphalt binder, σ_0 is the initial strass, $\Gamma(.)$ is the Gamma function, α and β are the fractional exponents, $\varepsilon_{\infty}^0(0)$ is the adjustment factor of Maxwell's model, $\varepsilon_M^0(0)$ is the adjustment factor of the parallel system, and t is the time.

3. Results and discussion

3.1. Rheological model for asphalt binders

To develop a rheological correlation using elastic-viscous models for the creep and recovery phenomena of binders and asphalt mixtures, a mechanical model was established (see Fig. 4) based on a rheological modification of the Burgers model [16,24,25]. The proposed model for asphalt binders was achieved by extracting the mechanical representation of the aggregate ξ_2 from the model proposed for asphalt mixtures [20]. The resulting model dif-

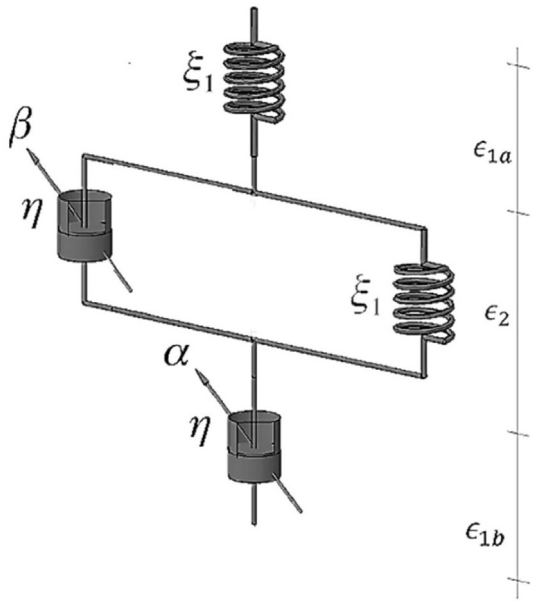

Fig. 4. Schematic diagram of the proposed model of asphalt binders.

fers from the one proposed by Burgers and other models because it has only two rheological constants (ξ_1 and η), representing the elasticity and viscosity of the asphalt binder. In this way, all deformation states of the asphalt binder can be explained, reducing the number of rheological variables involved in curve settings. The use of fractional exponents (α andβ) allows the elastic-viscous transition of the binders to be established since they are not considered Newtonian fluids at a temperature of 20 °C [3].

The percentage deformations of the recovery phenomenon in mixtures are first determined for each magnitude of load and type of binder used to establish the correlation between the rheological properties of binders and asphalt mixtures. Then, the MSCR test cycle is determined, which obtains the same percentage deformation compared to those of the mixture. A curve-fitting for the MSCR recovery phenomenon (see Eq. (3)) is then carried out, correlating the values of ξ_1 and η properties of the asphalt binder with both models (see Fig. 3). The recovery equation for the MSCR binder is given by (see Appendix A)

$$R_2(t) = \epsilon_M^0(0)\sum_{k=0}^{\infty}\frac{\left(-\frac{\xi_1}{\eta}t^{\beta}\right)^k}{\Gamma(1+\beta k)} + \epsilon_{\infty}^0(0), \tag{3}$$

where $R_2(t)$ is the recovery strain for asphalt binders, $\varepsilon_{\infty}^0(0)$ the fit factor from Maxwell's model, and $\varepsilon_M^0(0)$ the fit factor from the parallel system.

The model has a relaxation time [26] that depends exclusively on the properties defined by the asphalt binder (η, ξ_1), unlike Eq. (1) and Eq. (2), which have a relaxation time determined by the variables M and η, as it is typical of asphalt mixing.

3.2. Creep and recovery analysis for asphalt mixtures

The deformation that occurs when asphalt mix specimens are subjected to different magnitudes of loading depends on the type of binder used and its strength. In this respect, asphalt mixes will be directly influenced by the states of non-recoverable deformation due to the softening point of each asphalt binder (see Table 1). The conventional asphalt binders generate less thermal inertia, resulting in higher permanent strains. The asphalt mix with B70/100 (see Fig. 5b) achieves the most significant deformation over the entire range of the loads tested. The load of 6 kN creates a maximum creep deformation of 0.6 mm. However, this result is due to a higher activation energy, E_f, compared to the remaining binders [3]. This growth generates a more significant kinetic movement of the internal particles of the B70/100, causing the softening of the material with higher velocity. Secondly, the mixture manufactured with B50/70 (see Fig. 5a) exhibits lower deformation than B70/100 for a load of 6 kN due to a higher softening point of the binder. Finally, asphalt mixes with PMB 45/80-65 (see Fig. 5c) show lower deformation for 6 kN compared to mixes with conventional binders. This effect can be explained as a result of the incorporation of the rubber elastomer polymers in the modified binder, which changes the asphalt binder to reduce the heat generated by the loads, delaying the softening and plasticization of the mixture.

However, the results obtained (see Table 3) show that the instantaneous jump is directly proportional to the load magnitude when Eq. (1) is fitted to the experimental data from creep [20], since its determination is related to the ratio between the deformation and the force magnitudes. The mixtures with B70/100 show higher values of ξ_1 compared to those containing B50/70 due to the fact that the modulus of elasticity is inversely proportional to the elastic jump. Therefore, the mixture with B70/100 has a shorter linear viscoelastic deformation time. The asphalt mixture with PMB45/80-65 increases the elastic value to a maximum of ξ_1 = 7.238 MPa, indicating that the rubber polymer generates higher recoverable non-linear development.

A recoverable nonlinear elastic-viscous deformation starts after the first elastic jump, which is developed by the parallel system of the mentioned model of mixtures. The elastic jump that comes from this deformation establishes a value that adds up the elasticities of the asphalt binder and the aggregate. The curvature obtained experimentally is demonstrated by the Mittag-Leffler infinite series, symbolized by the fractional exponent. The value of this second elastic jump, M, and ξ_1 are used to obtain the average Youngs modulus of the aggregate of the mix, i.e., ξ_2 = 636.4 MPa. This result explains why the aggregate cannot be deformed in a mixture, delivering volumetric and load dissipation properties capable of increasing the second elastic jump and delaying the viscosity. The fractional exponent β remains approximately constant for conventional mixtures for loads of 3 kN, 4 kN, and 5 kN. Therefore, the magnitude of the load does not affect the transient behavior of the recoverable deformation before the constant slope is achieved (fractional exponent α). Mixtures with PMB45/80-65 have a transition from the elastic to viscous state that reaches higher values of β compared to conventional ones.

The last phase of creep is characterized by a straight line with a constant slope, generating non-linear and non-recoverable viscoelasticity. Each asphalt mix adopts a certain final deformation determined by the constants η and α, defined by the last damper of the model. The value of the parameter α decreases as the applied load increases. The mixtures with B70/100 have higher slopes, causing more significant non-recoverable deformations. The asphalt mixtures with B50/70 and PMB45/80-65 reach similar values of α, having lower viscous components compared to the B70/100 binder. Thus, the final strain of the asphalt mixes is mainly influenced by the rheological properties of the asphalt binder. It is necessary to obtain the rheological variables ξ_1 and η for each load magnitude to determine the final slope of the creep phenomenon, which governs the degree of final plasticity of the recovery phenomenon.

The recovery phenomenon that occurs when the load is removed shows the degree of plasticity caused in the creep process that leads to permanent deformation of the asphalt mix. When the strain is elastic, its recovery is complete, i.e., the mixing cylinder returns to its initial physical state. Out of the tests performed at 20 °C, none exhibits this condition, since both the overload and

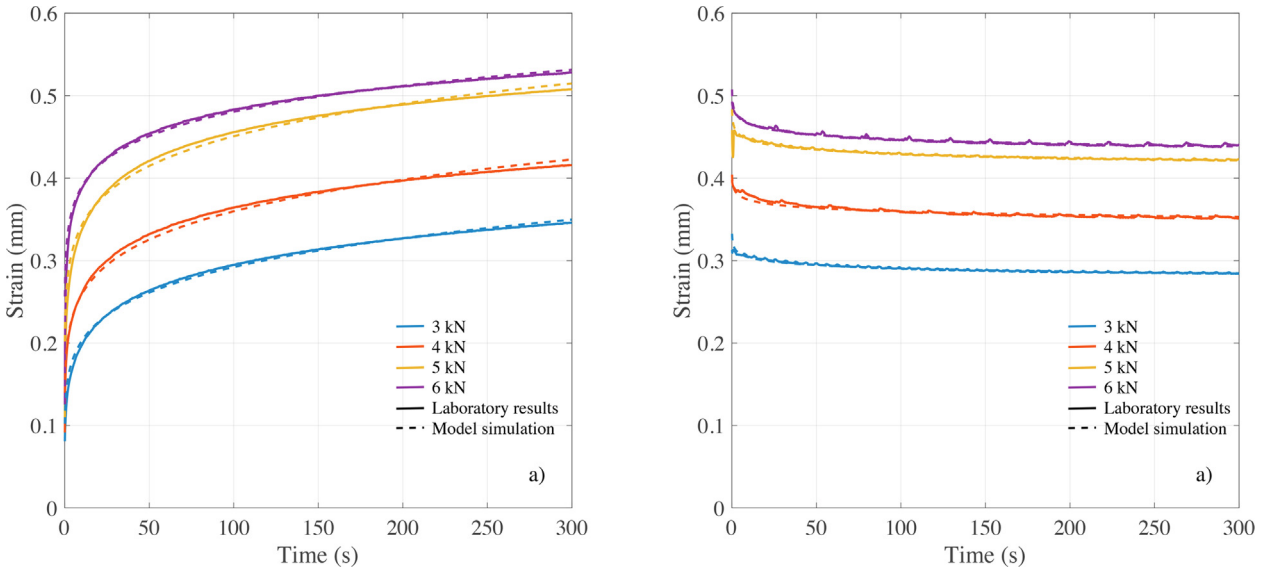

Fig. 5a. Creep-recovery test for asphalt mixture B50/70. Comparison between experimental data (solid line) and prediction (dashed line) at different load magnitudes is shown.

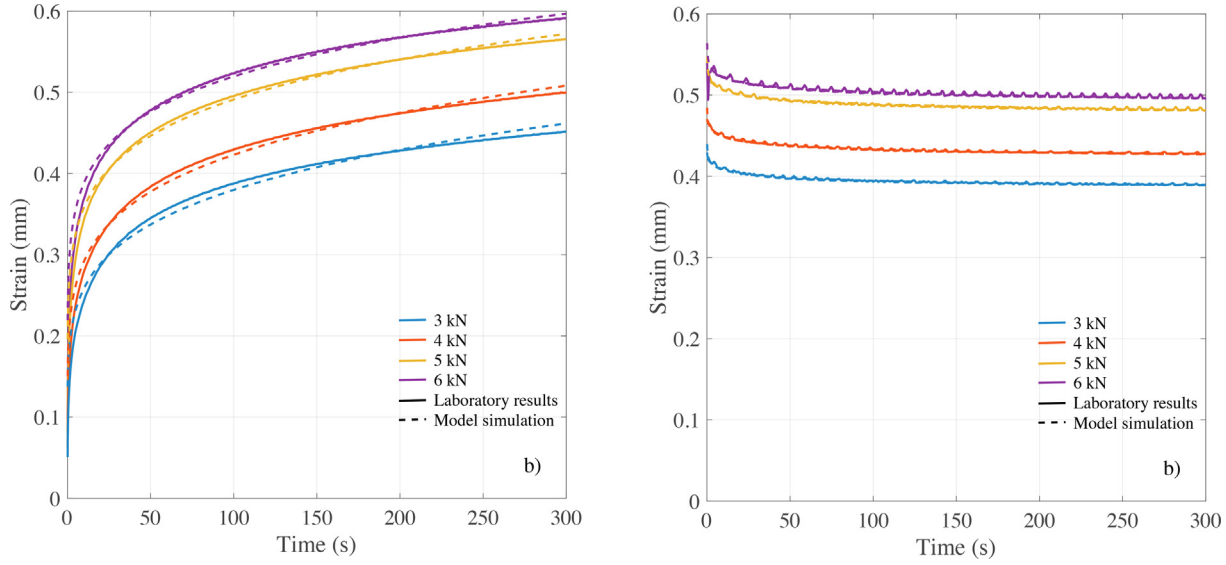

Fig. 5b. Creep-recovery test for asphalt mixture B70/100. Comparison between experimental data (solid line) and prediction (dashed line) at different load magnitudes is shown.

the load duration generate plastic deformations. Conventional mixtures recover less from strain at the end of each cycle compared to asphalt mixtures with a modified binder (see Fig. 5). Mixing with B70/100 binder produces a loss of 0.82% of the recovery for a load of 6 kN, obtaining a permanent deformation superior to that when mixing with B50/70, attaining a loss of 0.65% for the same load conditions. This corresponds to the presented analysis on the last creep phase since the curve-fitting determined higher values of α for the mixture with B70/100. Samples with PMB 45/80-65 achieved recovery from higher deformations due to a more top-elastic component (lower values of α) [3], causing a final permanent deformation of 0.54% for a load of 6 kN.

The recovery phenomenon showed through curve-fitting (see Eq. (2)) that the rheological properties of the aggregate and the asphalt binder remain the same as those obtained for the creep phenomenon. The constant β is of equal rheological value for both phenomena, showing the capacity of this model to predict the recovery phenomenon in the asphalt mixture. The curve-fitting established that PMB45/80-65 is the binder that recovers the most from deformation since it has a more significant development of the exponent β. The instantaneous elastic jump of the recovery ε_{∞}^{0} increases with the magnitude of the load, i.e., the mixtures with B70/100 reach a higher elastic jump of recovery, reaching a maximum value of 0.4831 mm for a load of 6 kN. After the elastic jump, a time-dependent recovery starts to develop, which is mathematically related to the multiplication of the infinite Mittag-Leffler series and the factor ϵ_{M}^{0}. The results indicate that the value of this factor is directly proportional to the load, and the infinite series maintains the values of the creep phenomenon.

The parameter α is not considered for the recovery phenomenon since its physical interpretation is based on the non-recoverable deformation. Therefore, an asphalt mix that obtains more significant development of the parameter β will have less plastic damage caused by permanent deformation failures. When

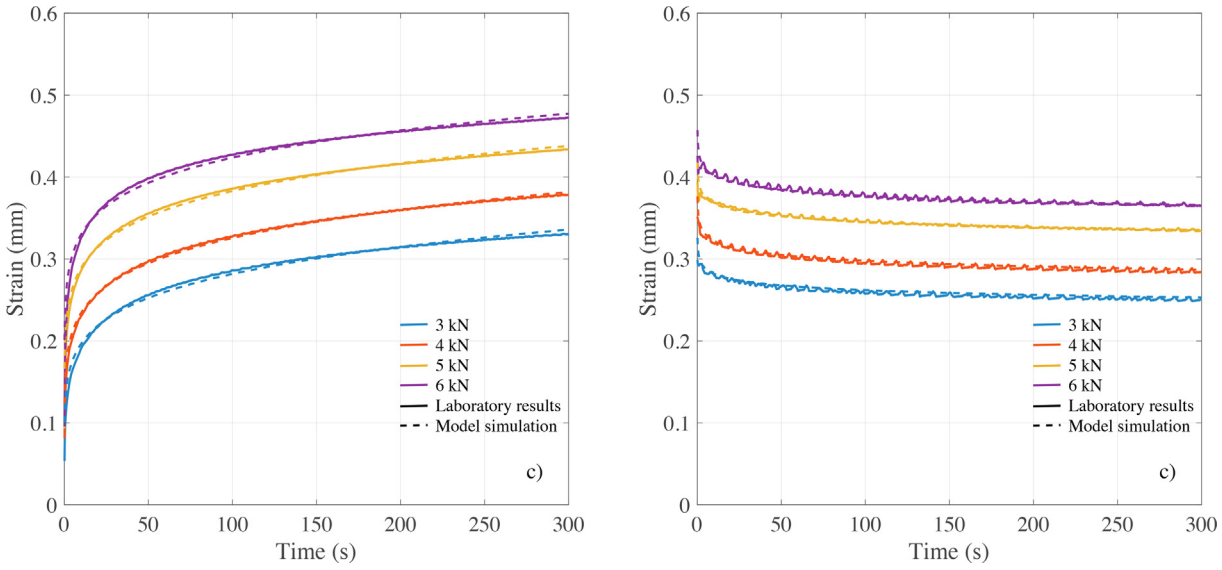

Fig. 5c. Creep-recovery test for asphalt mixture PMB45/80-65. Comparison between experimental data (solid line) and prediction (dashed line) at different load magnitudes is shown.

Table 3
Creep-recovery of asphalt mixtures for a temperature of 20 °C.

Type of binder	Load (kN)	ξ_1 (MPa)	ξ_2 (MPa)	η (MPa*s)	α	β	$\varepsilon^0_\infty(0)$ (mm)	$\varepsilon^0_M(0)$ (mm)	R^2
B 50/70	3	3.2700	639.7	7.5070	0.2656	0.1106	0.2441	7.1420	0.99
	4	4.3600	635.0	5.1990	0.1981	0.1200	0.2995	12.0900	0.99
	5	3.8710	635.0	4.6300	0.1639	0.1276	0.3790	13.5900	0.99
	6	5.9000	635.0	3.7870	0.1243	0.1288	0.3915	18.4500	0.98
B 70/100	3	4.7470	635.3	3.6700	0.2221	0.1200	0.3533	13.6000	0.99
	4	6.6700	637.7	3.7380	0.1996	0.1200	0.3866	15.3200	0.99
	5	6.6670	635.0	3.6750	0.1770	0.1525	0.4478	15.9100	0.99
	6	9.000	635.0	3.6750	0.1586	0.2763	0.4831	15.9100	0.98
PMB 45/80-65	3	4.1180	640.0	5.9900	0.2344	0.0900	0.1784	14.0000	0.98
	4	4.9980	639.0	5.9980	0.2087	0.1203	0.2243	14.4600	0.98
	5	7.2380	635.0	4.4240	0.1565	0.3190	0.3270	14.4600	0.99
	6	7.2000	635.0	4.2400	0.1278	0.3955	0.3634	16.6300	0.99

varying the magnitude of the load, conventional mixes tend to keep the parameter β constant, since the physical transformation of the asphalt binder is fast, creating more work from the fractional exponent α. The mixtures with the modified binder increase the value of β because of the slow transformation of the asphalt binder, exhibiting lower values of non-recoverable deformations. The rheological properties ξ_1, ξ_2, and η obtained in the load-unload cycles are kept constant throughout the whole process of creep and recovery cycles for each binder and aggregate.

3.3 . Correlation of creep and recovery analyses for asphalt mixes and binders

Creep and recovery analyses for conventional and modified binders were carried out using a dynamic shear rheometer (DSR) to correlate the data provided by the asphalt mix simulation. The MSCR test generates deformations in asphalt binder samples through multiple cycles of angular torsional stress. The correlation of the rheological properties of binders and asphalt mixtures was carried out only for recovery phenomena for percentage deformations at a temperature of 20 °C.

In Fig. 6a, the multiple deformations of the three binders mentioned for the MSCR test are shown. It can be seen that the B70/100 binder is the one that exhibits the highest accumulated strain over the 10 cycles, ending with a deformation of 1.72%, which ratifies the behavior that occurred in the asphalt mixtures. B50/70 binder

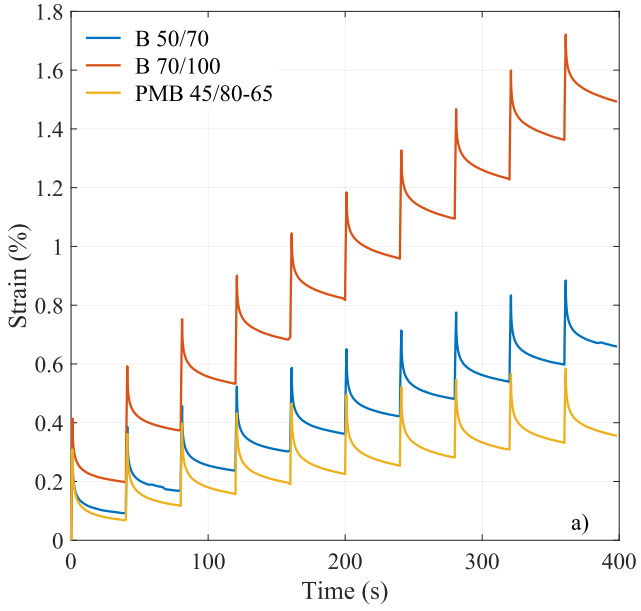

Fig. 6a. MSCR tests for binders.

Table 4
Recovery of asphalt binder at a temperature of 20 °C.

Type of binder	No. of cycles	ξ_1 (MPa)	η (MPa*s)	β	$\varepsilon^0_\infty(0)$ (mm)	$\varepsilon^0_M(0)$ (mm)	R^2
B 50/70	5	3.2700	7.5070	0.1106	0.2441	7.1420	0.99
	6	4.3600	5.1990	0.1200	0.2995	12.0900	0.94
	8	3.8710	4.6300	0.1276	0.3790	13.5900	0.93
	9	5.9000	3.7870	0.1288	0.3915	18.4500	0.91
B 70/100	4	4.7470	3.6700	0.1200	0.3533	13.6000	0.85
	4	6.6700	3.7380	0.1200	0.3866	15.3200	0.89
	5	6.6670	3.6750	0.1525	0.4478	15.9100	0.89
	6	9.000	3.6750	0.2763	0.4831	15.9100	0.88
PMB 45/80-65	7	4.1180	5.9900	0.0900	0.1784	14.0000	0.98
	8	4.9980	5.9980	0.1203	0.2243	14.4600	0.98
	9	7.2380	4.4240	0.3190	0.3270	14.4600	0.89
	10	7.2000	4.2400	0.3955	0.3634	16.6300	0.89

displays a lower plastic deformation compared to B70/100, reaching a maximum of 0.87% in accumulated strain. PMB45/80-65 binder preserves its strain in a lower range due to the aggregate polymers and its maximum deformation does not exceed 0.60%.

The curve-fitting analysis of the MSCR test was considered with the model intended for asphalt binders (see Eq. (3)). No curve-fitting was carried out in the case of creep deformation, as the curves obtained in the rheometer show no apparent difference in the recoverable and non-recoverable states for 1 s, caused by the viscous component of the asphalt binders. The simulation results for asphalt binders are summarized in Table 4. The simulation values are related to the number of cycles depending on the type of asphalt binder, with a higher number of cycles resulting in a lower softening point (see Table 1). The rheological properties of the asphalt binders, ξ_1, and η, remain both the same as for the previous calculations in asphalt mixtures ($R^2 > 0.85$). This means that there is a good correlation between the proposed model for asphalt mixes and binders and the experimental data.

Fig. 6b shows the recovery of the binder B50/70 by correlating the number of cycles with the load magnitude. The ninth period induced by the rheometer showed the same recovery deformation as applying a 6 kN load to an asphalt mix. Curve-fitting shows that the fractional operator β remains constant from the third to the eighth cycle and then increases its value to generate a slower rate of change, causing more significant plastic deformation. The number of cycles required to match the rheological values obtained in mixtures and binders is lower for the B70/100 binder compared to the B50/70 binder (see Fig. 6c), due to the increase in plastic deformation and a percentage increase in the non-recoverable deformation stage. For a load of 6 kN, the average strain is 0.1%, which is achieved in the fifth cycle of the MSCR test.

The percentage deformation of asphalt mixtures containing PMB45/80-65 binders (see Fig. 6d) does not cause the same abrupt changes as with conventional asphalt binders. The ratio between the tests is achieved with subsequent cycles, as the polymer-based asphalt binder generates a lower plastic deformation. The range of deformation is lower than that for conventional binders, and the curve-fitting is achieved with a strain of approximately 0.8%, using up to the 10th cycle of the MSCR test. The use of polymers in binders generates a better effect for permanent deformations compared to the use of conventional asphalt binders, due to the ability of polymers to delay the viscoelastic-to-viscous transformation process of the binder [3]. It can also be mentioned that the number of tests in asphalt mixtures could be reduced using the rheological asphalt-binder analysis. The rheological analysis in asphalt binders can predict a deformation domain in asphalt mixtures if the modulus of elasticity of the mineral skeleton is known.

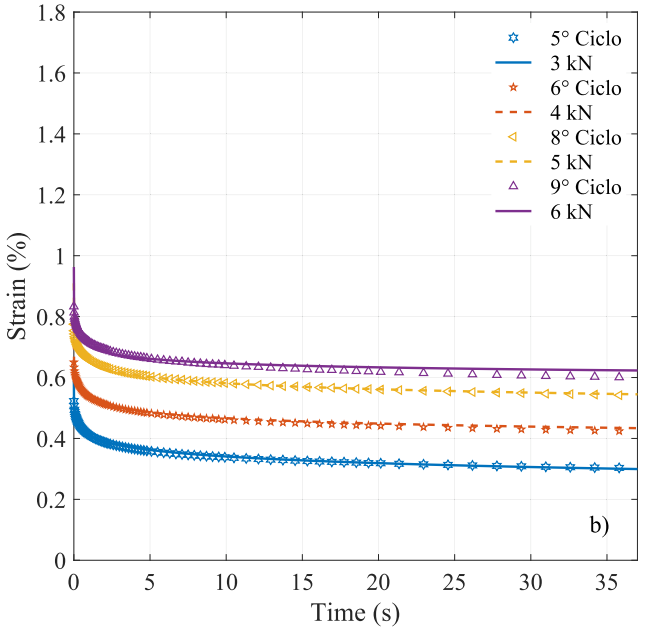

Fig. 6b. MSCR tests for B50/70 binder. Comparison between experimental data (solid line) and predictions (dashed line) at different loads and number of cycles.

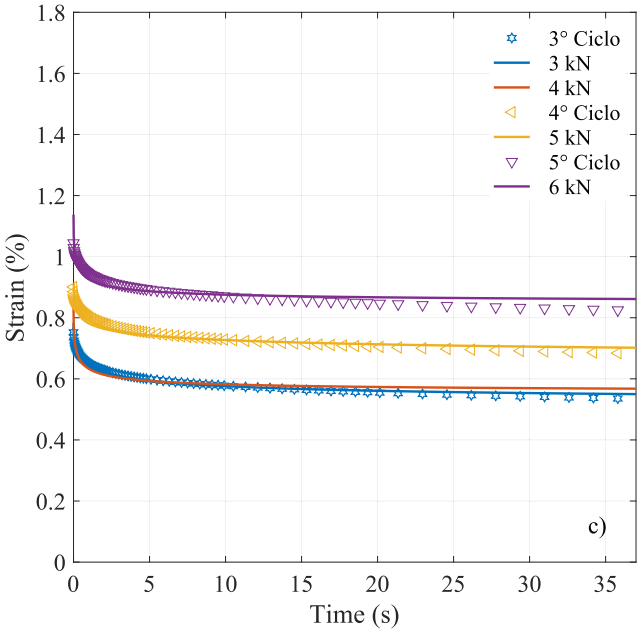

Fig. 6c. MSCR tests for B70/100 binder. Comparison between experimental data (solid line) and predictions (dashed line) at different loads and number of cycles.

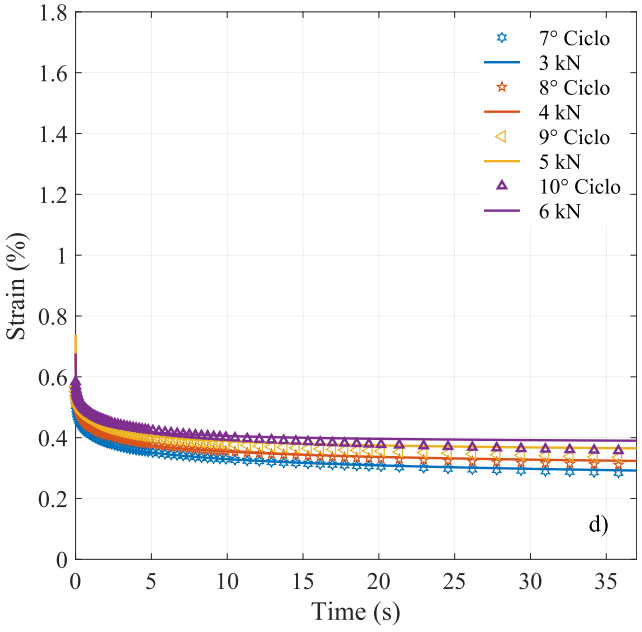

Fig. 6d. MSCR tests for PMB 45/80-65 binder. Comparison between experimental data (solid line) and predictions (dashed line) at different loads and number of cycles.

4. Conclusions

Based on the results obtained in this research, the following conclusions are drawn:

The model allows the curve-fitting of experimental data for permanent deformations. It provides rheological values for the asphalt binder (ξ_1 and η) and the aggregate used (ξ_2). This model reduces the number of rheological constants compared to other classical models, allowing the fractional exponents to describe the physical significance of transition between the elastic and viscous state of the material.

The proposed methodology allows the correlation through mechanical models of the permanent deformations that occur in asphalt mixtures and binders based on the uniaxial compression test and MSCR, respectively, generating details of the creep and recovery phenomena for the prediction of permanent deformations in both mixtures and binders.

The behavior of the conventional mixtures under the different values of loads used generated higher permanent deformations with the B70/100 binder, since it has a lower softening point than B50/70 and makes strains in the non-recoverable range of the creep phenomenon, causing an increase in the fractional parameter α.

The mixtures with the PMB45/80-65 binder obtained the lowest plastic deformations due to their rheological properties generating more significant strain in the recoverable range (increase in the parameter β). This is due to its ability to decrease softening due to the delayed kinetic movement of the binder particles produced by the added polymers.

Further work is planned to compare the methodology outlined in this paper with fatigue failure and permanent deformation experimental tests of mastic asphalt under dynamic loads.

CRediT authorship contribution statement

M. Lagos-Varas: Conceptualization, Methodology, Formal analysis, Software, Writing - original draft. **A.C. Raposeiras:** Methodology, Data curation, Writing - review & editing. **D. Movilla-Quesada:** Visualization, Supervision, Project administration. **J.P. Arenas:** Writing - review & editing. **D. Castro-Fresno:** Resources, Supervision. **O. Muñoz-Cáceres:** Formal analysis, Methodology. **V.C. Andres-Valeri:** Validation.

Declaration of Competing Interest

The authors declare that they have no known competing financial interests or personal relationships that could have appeared to influence the work reported in this paper.

Acknowledgements

This research was funded by ANID/CONICYT though the project FONDECYT Regular N° 1201029. The authors gratefully acknowledge the institutional support provided by the Vice-Rectory for Research, Development and Artistic Creation of the University Austral of Chile (VIDCA UACh) and to the Santander Bank Iberoamerican Scholarship Program, which made it possible to carry out this research. The authors would also like to thank the GITECO and GCS research groups from the University of Cantabria (Spain) for their support.

Appendix A

The total system deformation shown in Fig. 4 is given by

$$\epsilon = \epsilon_{1a} + \epsilon_2 + \epsilon_{1b} \tag{A1}$$

The fractional differential equations are given by

$$D_t^{\alpha}\epsilon_{1a+1b} = \frac{1}{\xi_1} D_t^{\gamma}\sigma(t) + \frac{1}{\eta}\sigma(t) \tag{A2}$$

and

$$D_t^{\beta}\epsilon_2(t) = \frac{1}{\eta}\sigma(t) - \frac{\xi_1}{\eta}\epsilon_2(t) \tag{A3}$$

Taking the fractional derivative $\alpha + \beta$ of Eq. (A1) to time,

$$D_t^{\alpha+\beta}\epsilon(t) = D_t^{\alpha+\beta}\epsilon_{1a+1b} + D_t^{\alpha+\beta}\epsilon_2 \tag{A4}$$

Now, taking the fractional-order derivative β from Eq. (A2) and the order α from Eq. (A3), we get

$$D_t^{\alpha+\beta}\epsilon_{1a+1b}(t) = \frac{1}{\xi_1} D_t^{\gamma+\beta}\sigma(t) + \frac{1}{\eta} D_t^{\beta}\sigma(t) \tag{A5}$$

and

$$D_t^{\alpha+\beta}\epsilon_2(t) = \frac{1}{\eta} D_t^{\alpha}\sigma(t) - \frac{\xi_1}{\eta} D_t^{\alpha}\epsilon_2 \tag{A6}$$

Substituting Eqs. (A5) and (A6) in Eq. (A4), we get

$$D_t^{\alpha+\beta}\epsilon(t) = \frac{1}{\xi_1} D_t^{\gamma+\beta}\sigma(t) + \frac{1}{\eta} D_t^{\beta}\sigma(t) + \frac{1}{\eta} D_t^{\alpha}\sigma(t) - \frac{\xi_1}{\eta} D_t^{\alpha}\epsilon_2 \tag{A7}$$

To express Eq. (A7) as a function of total deformation, we take the fractional-order derivative α of Eq. (A1) to time:

$$D_t^{\alpha}\epsilon = D_t^{\alpha}\epsilon_{1a+1b} + D_t^{\alpha}\epsilon_2 \tag{A8}$$

Solving $D_t^{\alpha}\varepsilon_2$ in Eq. (A8) and using Eq. (A2) gives the following equation:

$$D_t^{\alpha+\beta}\epsilon + \frac{(\xi_1)}{\eta} D_t^{\alpha}\epsilon = \frac{1}{\xi_1} D_t^{\beta+\gamma}\sigma + \frac{1}{\eta} D_t^{\beta}\sigma + \frac{1}{\eta} D_t^{\alpha}\sigma + \frac{1}{\eta} D_t^{\gamma}\sigma + \frac{\xi_1}{\eta^2}\sigma \tag{A9}$$

The total recovery function for asphalt binders is obtained by eliminating the concept of initial load σ_0 and applying the Laplace transform:

$$\widehat{\epsilon}(s)\left[s^{\alpha+\beta}-\sum_{k=0}^{m-1}s^{\alpha+\beta-k-1}\epsilon^{k}(0)+\frac{\xi_1}{\eta}s^{\alpha}-\sum_{k=0}^{m-1}s^{\beta-k-1}\epsilon^{k}(0)\right]=0 \qquad 10)$$

Note that the fractional α and β can reach maximum values of 1, then m−1 = *0*. Therefore, the sums in Eq. (A10) are cancelled, and only the initial conditions of deformation remain. Using first the Maxwell model and later the kelvin-Voigt model, we obtain

$$R_2(t)=\epsilon_M^0(0)\sum_{k=0}^{\infty}\frac{\left(-\frac{\xi_1}{\eta}t^{\beta}\right)^{k}}{\Gamma(1+\beta k)}+\epsilon_{\infty}^0(0) \qquad 11)$$

References

[1] P. Ahmedzade, K. Demirelli, T. Günay, F. Biryan, O. Alqudah, Effects of waste polypropylene additive on the properties of bituminous binder, Procedia Manuf. 2 (2015) 165–170, https://doi.org/10.1016/j.promfg.2015.07.029.

[2] J. Zhang, G.S. Simate, X. Hu, M. Souliman, L.F. Walubita, Impact of recycled asphalt materials on asphalt binder properties and rutting and cracking performance of plant-produced mixtures, Constr. Build. Mater. 155 (2017) 654–663, https://doi.org/10.1016/j.conbuildmat.2017.08.084.

[3] M. Lagos-varas, D. Movilla-quesada, A.C. Raposeiras, J.P. Arenas, M.A. Calzada-pérez, A. Vega-Zamarillo, P. Lastra-González, Influence of limestone filler on the rheological properties of bituminous mastics through susceptibility master curves, Constr. Build. Mater. 231 (2020) 117126, https://doi.org/10.1016/j.conbuildmat.2019.117126.

[4] Z. Yao, J. Zhang, F. Gao, S. Liu, T. Yu, Integrated utilization of recycled crumb rubber and polyethylene for enhancing the performance of modified bitumen, Constr. Build. Mater. 170 (2018) 217–224, https://doi.org/10.1016/j.conbuildmat.2018.03.080.

[5] D. Ge, Z. You, S. Chen, C. Liu, J. Gao, The performance of asphalt binder with trichloroethylene: improving the efficiency of using reclaimed asphalt pavement, J. Clean. Prod. 232 (2019) 205–212, https://doi.org/10.1016/j.jclepro.2019.05.164.

[6] M. Baqersad, H. Ali, Rheological and chemical characteristics of asphalt binders recycled using different recycling agents, Constr. Build. Mater. 228 (2019) 116738, https://doi.org/10.1016/j.conbuildmat.2019.116738.

[7] B. Singh, P. Kumar, Effect of polymer modification on the ageing properties of asphalt binders: chemical and morphological investigation, Constr. Build. Mater. 205 (2019) 633–641, https://doi.org/10.1016/J.CONBUILDMAT.2019.02.050.

[8] S. Mangiafico, H. Di Benedetto, C. Sauzéat, F. Olard, S. Pouget, L. Planque, Relations between linear ViscoElastic behaviour of bituminous mixtures containing reclaimed asphalt pavement and colloidal structure of corresponding binder blends, Procedia Eng. 143 (2016) 138–145, https://doi.org/10.1016/j.proeng.2016.06.018.

[9] A. Diab, Z. You, X. Li, J. Carvalho, X. Yang, S. Chen, Rheological models for non-newtonian viscosity of modified asphalt binders and mastics, Egypt. J. Pet. (2019), https://doi.org/10.1016/j.ejpe.2019.12.002.

[10] D. Yu, Y. Gu, X. Yu, Rheological-microstructural evaluations of the short and long-term aged asphalt binders through relaxation spectra determination, Fuel. 265 (2020) 116953, https://doi.org/10.1016/j.fuel.2019.116953.

[11] Y. Sun, W. Wang, J. Chen, Investigating impacts of warm-mix asphalt technologies and high reclaimed asphalt pavement binder content on rutting and fatigue performance of asphalt binder through MSCR and LAS tests, J. Clean. Prod. 219 (2019) 879–893, https://doi.org/10.1016/j.jclepro.2019.02.131.

[12] J. Zhang, L.F. Walubita, A.N.M. Faruk, P. Karki, G.S. Simate, Use of the MSCR test to characterize the asphalt binder properties relative to HMA rutting performance – a laboratory study, Constr. Build. Mater. 94 (2015) 218–227, https://doi.org/10.1016/j.conbuildmat.2015.06.044.

[13] X. Yang, Z. You, High temperature performance evaluation of bio-oil modified asphalt binders using the DSR and MSCR tests, Constr. Build. Mater. 76 (2015) 380–387, https://doi.org/10.1016/j.conbuildmat.2014.11.063.

[14] Q. Lv, W. Huang, H. Sadek, F. Xiao, C. Yan, Investigation of the rutting performance of various modified asphalt mixtures using the Hamburg wheel-tracking device test and multiple stress creep recovery test, Constr. Build. Mater. 206 (2019) 62–70, https://doi.org/10.1016/j.conbuildmat.2019.02.015.

[15] T. Ma, H. Wang, D. Zhang, Y. Zhang, Heterogeneity effect of mechanical property on creep behavior of asphalt mixture based on micromechanical modeling and virtual creep test, Mech. Mater. 104 (2017) 49–59, https://doi.org/10.1016/j.mechmat.2016.10.003.

[16] P.K. Ashish, D. Singh, Effect of carbon nano tube on performance of asphalt binder under creep-recovery and sustained loading conditions, Constr. Build. Mater. 215 (2019) 523–543, https://doi.org/10.1016/j.conbuildmat.2019.04.199.

[17] P.E. Rong Lou, H. Liu, Y. Zhang, Characterization of linear viscoelastic, nonlinear viscoelastic and damage stages of asphalt mixtures, Constr. Build. Mater. 125 (2016) 72–80, https://doi.org/10.1016/j.conbuildmat.2016.08.039.

[18] Y. Lei, H. Wang, X. Chen, X. Yang, Z. You, S. Dong, J. Gao, Shear property, high-temperature rheological performance and low-temperature flexibility of asphalt mastics modified with bio-oil, Constr. Build. Mater. 174 (2018) 30–37, https://doi.org/10.1016/j.conbuildmat.2018.04.094.

[19] P. Li, X. Jiang, K. Guo, Y. Xue, H. Dong, Analysis of viscoelastic response and creep deformation mechanism of asphalt mixture, Constr. Build. Mater. 171 (2018) 22–32, https://doi.org/10.1016/j.conbuildmat.2018.03.104.

[20] M. Lagos-Varas, D. Movilla-Quesada, J.P. Arenas, A.C. Raposeiras, D. Castro-Fresno, M.A. Calzada-Pérez, A. Vega-Zamanillo, J. Maturana, Study of the mechanical behavior of asphalt mixtures using fractional rheology to model their viscoelasticity, Constr. Build. Mater. 200 (2019) 124–134, https://doi.org/10.1016/j.conbuildmat.2018.12.073.

[21] M. Han, J. Li, Y. Muhammad, D. Hou, F. Zhang, Y. Yin, S. Duan, Effect of polystyrene grafted graphene nanoplatelets on the physical and chemical properties of asphalt binder, Constr. Build. Mater. 174 (2018) 108–119, https://doi.org/10.1016/j.conbuildmat.2018.04.082.

[22] F. Lorenzo, T.T. Hartley, R-Function Relationships in the Fractional Calculus for Application, National Aeronautics and Space Administration, Glenn Research Center, 2000. NASA/TM-2000-210361.

[23] M. Vila-Cortavitarte, P. Lastra-González, M.A. Calzada-Pérez, I. Indacoechea-Vega, The use of recycled plastic as partial replacement of bitumen in asphalt concrete, Use Recycl. Plast. Eco-Efficient Concr. (2019) 327–347, https://doi.org/10.1016/b978-0-08-102676-2.00015-3.

[24] N. Saboo, P. Kumar, A study on creep and recovery behavior of asphalt binders, Constr. Build. Mater. 96 (2015) 632–640, https://doi.org/10.1016/j.conbuildmat.2015.08.078.

[25] G. Dondi, V. Vignali, M. Pettinari, F. Mazzotta, A. Simone, C. Sangiorgi, Modeling the DSR complex shear modulus of asphalt binder using 3D discrete element approach, Constr. Build. Mater. 54 (2014) 236–246, https://doi.org/10.1016/j.conbuildmat.2013.12.005.

[26] E. Pierro, L. Afferrante, G. Carbone, On the peeling of elastic tapes from viscoelastic substrates: designing materials for ultratough peeling, Tribol. Int. (2020) 106060, https://doi.org/10.1016/j.triboint.2019.106060.